Nature of defects and their relationship with the growth and properties of diamond films

R. C. Hyer, M. Green,* and S. C. Sharma†
Department of Physics, The University of Texas at Arlington, Arlington, Texas 76019
(Received 1 December 1993)

We present results for the lattice defects in diamond films and discuss interplay between the defects and growth rate of the films grown by chemical vapor deposition and dc plasma arc jet. We identify the nature of the defects and present defect depth profiles for films grown under different conditions of these two techniques. Defect density and film properties change significantly with growth parameters and the growth rate is related to defects in the film.

I. INTRODUCTION

Diamond films grown by chemical vapor deposition (CVD) have attracted worldwide attention because of their technological importance and fascination from a scientific point of view.[1] Whereas significant progress has been made in understanding the nucleation, growth, and properties of such films, very little is known about defects and their role in the properties of diamond films. Most of the defects are introduced in the films during the growth process and they should influence both the growth and the ultimate properties of these films. We have characterized diamond films by scanning tunneling microscopy,[2] scanning electron microscopy,[3] Raman spectroscopy,[4] x-ray photoelectron spectroscopy,[5] and positron lifetime spectroscopy.[6] Here we present detailed results on microscopic defects in diamond films grown by the hot-filament-assisted chemical vapor deposition (HFCVD) and plasma arc jet techniques. These results are obtained by utilizing Raman spectroscopy and three standard techniques of positron annihilation spectroscopy (variable energy positron beam, positron lifetime, and Doppler broadening). This combination of two defect-sensitive techniques allows us to identify defects (e.g., monovacancy vs microvoids), obtain depth profile and density of defects, and study correlations between the growth rate and quality (sp^3 vs sp^2 bonding) of the films. Diamond films grown for two different regimes of HFCVD exhibit a remarkably different depth profile of defects. Between the HFCVD and plasma arc jet films, the defect depth profiles are markedly different. In the case of the plasma arc jet films, defect profiles vary depending on whether the films are transparent or opaque. To our knowledge, these are the first detailed results that identify the nature of microscopic defects in diamond films and address an interplay between defects and film growth as well as properties of the films. Previous positron studies have provided limited results on defects; among these are micropores of diameter ~ 0.5 nm from the pulsed positron beam measurements on one a-C:H film,[7] defect concentrations ranging from 4×10^{-4} to 4×10^{-3} in three microwave plasma grown films,[8] vacancy and vacancy clusters in B-doped CVD films from positron lifetime measurements,[9] and positron lifetime and Doppler broadening measurements on CVD film.[6]

II. EXPERIMENTAL DETAILS

The HFCVD system used in these experiments has been discussed elsewhere.[4] It consists of a reaction chamber, a system for mixing and flow control of the hydrocarbon-hydrogen mixture, and instrumentation for the control and measurements of pressure, vacuum, and substrate temperature. Diamond films were grown for two different sets of parameters: (a) regime 1: filament temperature = 2000 K, substrate temperature = 1100 K, CH_4/H_2 flow rate = 350 SCCM (SCCM denotes cubic centimeter per minute at STP), and system pressure = 25 Torr; (b) regime 2: filament temperature = 2300 K, substrate temperature = 1100 K, CH_4/H_2 flow rate = 60 SCCM, and system pressure = 25 Torr. Our Raman spectrometer consists of an argon ion laser ($\lambda=5145$ Å), a SPEX model 14018 double monochromator, and computer control data acquisition. The spectrometer resolution ranged from 0.5 to 4 cm^{-1}. A JOEL model JSM 35-C scanning electron microscope was used to observe and photograph the surface morphology of the films. Our variable energy positron beam spectrometer utilizes a magnetically guided beam of low-energy (≤ 10 eV) positrons that are obtained from a ^{22}Na radioisotope and moderated by an annealed tungsten moderator. The moderated positrons are focused, transported in a high-vacuum system, and accelerated to desired kinetic energies up to 25 keV prior to being implanted into the sample. The 0.511-MeV γ rays, resulting from the annihilations of the positron-electron pairs, are collected with a high-purity Ge solid-state detector spectrometer. The energy resolution of this spectrometer is 1.14 keV at the 0.511 MeV annihilation γ-ray energy. The positron lifetime spectra are measured with a standard fast-fast timing spectrometer with a timing resolution of about 0.300 ns. These spectra are resolved into four exponential components by deconvoluting spectrometer resolution by using the POSITRONFIT–EXTENDED computer program.[10] The decay rate of each of these exponential components represents the "local" electron density in the microscopic region from which the positrons annihilate. The basic details of the interactions of the low-energy positrons in materials are discussed elsewhere.[11] Here it suffices to mention that positrons are trapped by lattice defects and that the annihilation characteristics of the trapped posi-

0163-1829/94/49(20)/14573(9)/$06.00

trons (e.g., lifetime and Doppler broadening in the annihilation gamma ray energy) are significantly different from those of the positrons that annihilate from defect-free regions in the test material.

III. RESULTS AND DISCUSSION

Raman and SEM

Raman spectroscopy is the most widely used technique for characterizing diamond films. This technique yields information about the relative sp^3 (diamond) vs sp^2 (graphitic) bonding and defects within the crystallites or grains in the films.[12] Raman spectra for selected diamond films from regimes 1 and 2 and plasma arc jet are shown in Fig. 1. These spectra exhibit three important features: (1) a sharp peak at 1332 cm^{-1} which is characteristic of crystalline diamond, (2) a broad peak centered at 1550 cm^{-1} which is characteristic of diamondlike carbon, and (3) peaks at approximately 1350 and 1580 cm^{-1} that are characteristic of polycrystalline graphite. An evolution from the sp^3 bonding to sp^2 bonding with increasing methane concentration is clearly seen for HFCVD samples. The characteristic that is most relevant to the microstructure/defects in these films is the full width at half maximum (FWHM) of the diamond peak. A broadening in the 1332-cm^{-1} diamond line has been shown to be related to an increase in defect density. These defects, which effectively decrease the size of the domains (defect-free regions) within the crystallites, may arise from increased nucleation density and from sp^2-bonded carbon dispersed within the diamond phase in the form of defects.[13] Table I shows our results for the FWHM of the 1332-cm^{-1} Raman line, domain sizes, and typical growth rates for these films. We show in Fig. 2 the relationship between the diamond content in the film vs the FWHM of the 1332-cm^{-1} diamond line in the Raman spectrum for all of our diamond films, including those grown under regimes 1 and 2, grown by the plasma arc technique, and natural diamond. We calculate the diamond content of the film from the ratio of the area under the 1332-cm^{-1} line to the total area under the entire spectrum from 1100 to 1700 cm^{-1}. The area calculation is done after correcting for the luminescence background. In addition, the scattering efficiency for the nondiamond component of the film is assumed to be 50 times higher than that for diamond.[4] It is interesting to note that the data for all these films, which were deposited under very different conditions of the HFCVD and also grown by utilizing a very different technique of plasma arc jet, follow a smooth "universal" curve. In the following, we correlate these results with the defect properties obtained from the positron annihilation measurements. The results of the Raman scans are in agreement with the typical SEM micrographs shown in Fig. 3. These micrographs clearly show that the films, exhibiting a well-resolved and relatively narrow 1332-cm^{-1} diamond line, contain well-faceted diamond crystals. The surface morphology of the films changes with variations in the deposition parameters: Whereas well-faceted and densely packed diamond crystallites are observed in films grown for low CH_4 concentrations in both *regimes*, spherical ball-shaped features dominate in the films grown for higher CH_4 concentrations. We have published elsewhere details on the nucleation and surface morphology of diamond films grown under both regimes.[3]

Defect depth profiles in the near-surface region

The variable energy positron beam is a powerful surface probe that enables depth profiling of defects in thin films.[11] The data from these experiments, conducted by implanting monoenergetic positrons at varying depths,[14] are analyzed by solving the positron diffusion equation.[15] This provides results for the positron diffusion length which changes because of positron trapping in defects. The depth profile of the defects is represented by the S parameter (equal to the area under a central narrow region divided by the total area under the annihilation energy peak after background correction), which is shown in Fig. 4. This parameter is sensitive to defects and to changes in the valence electron distribution. Among the regime-1 films, the 0.25% CH_4 film shows the lowest density of defects and the sharpest diamond peak in the Raman spectrum. There is a significant difference between the depth profiles of the two regime-1 films: The S parameter for the 0.25% CH_4 film is lower than that in the 2.0% CH_4 film. Similarly, among the regime-2 films, the 1.0% CH_4 film shows the lowest density of defects and the sharpest 1332-cm^{-1} Raman line. Between the highest quality film from regime 1 (0.25% CH_4) and the highest quality film from regime 2 (1% CH_4), the 0.25% CH_4 film has a much lower density of defects in the top 700 Å. The defect density gradually increases towards a

TABLE I. Results from Raman and growth rate analyses.

	CH_4 concentration (%)	FWHM of diamond peak (cm^{-1})	Domain size (nm)	Growth rate (μm/h)
Regime 1	0.25	5.6	12.7	0.3
	2.0	NA	NA	>0.3
Regime 2	1.0	10.2	6.8	0.6
	4.0	NA	NA	>0.6
Plasma	White	3.1	22.4	50
	Black	4.1	16.9	>50

value observed in the 1% CH_4 film. The 0.25% CH_4 film is, therefore, characterized by a slower growth rate, a sharper Raman line at 1332 cm^{-1}, and a lower density of defects. The plasma arc jet film, on the other hand, is characterized by a much higher growth rate, a much sharper 1332-cm^{-1} Raman line, and a much lower density of defects.

We obtain quantitative information about the density of defects in the top 1- to 2-μm of the films by fitting the S parameter vs positron implantation energy data to the

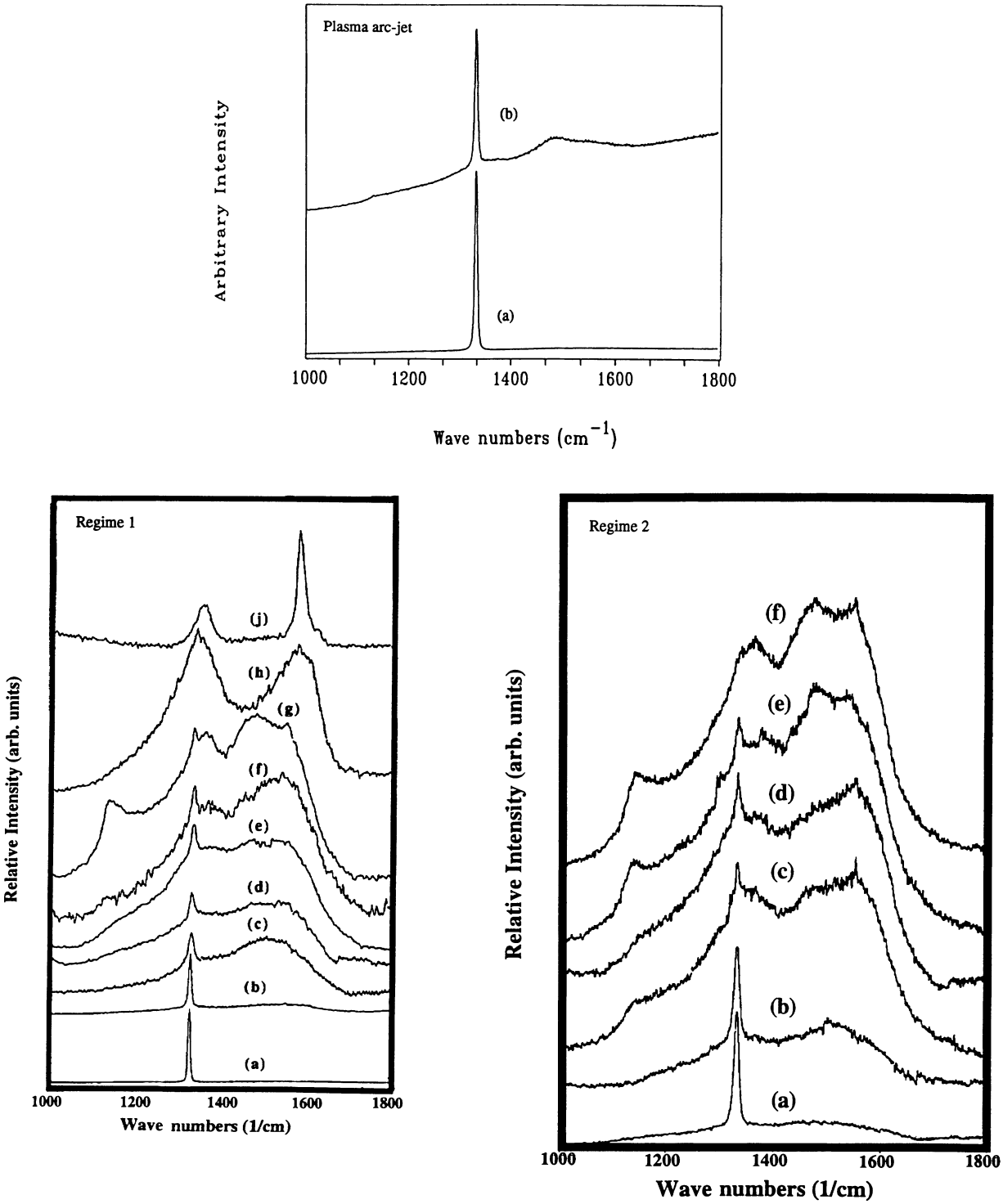

FIG. 1. Raman spectra of diamond films grown by HFCVD and plasma arc jet. Regime 1: (a) natural diamond, (b) 0.25% CH_4, (c) 0.5% CH_4, (d) 0.75% CH_4, (e) 1% CH_4, (f) 1.2% CH_4, (g) 1.4% CH_4, (h) 2% CH_4, and (j) grafoil. Regime 2: (a) 1% CH_4, (b) 2% CH_4, (c) 2.5% CH_4, (d) 2.75% CH_4, (e) 3% CH_4, and (f) 4% CH_4. Plasma arc jet: (a) white diamond and (b) black diamond.

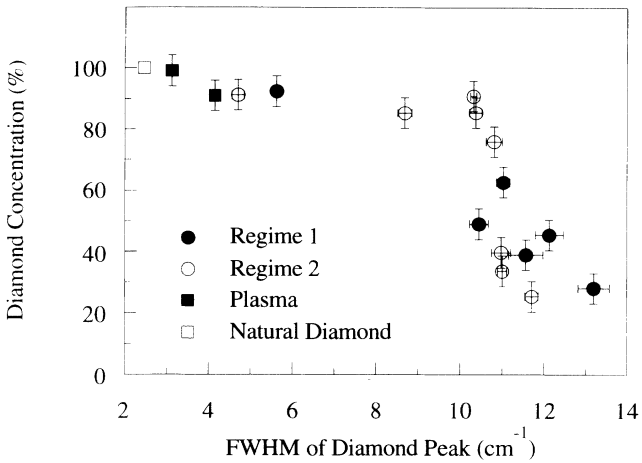

FIG. 2. Diamond content vs FWHM of the 1332-cm^{-1} Raman line for samples grown for conditions of regime 1, regime 2, plasma arc jet, and natural diamond.

one-dimensional positron diffusion equation:[15]

$$D_+ d^2c(z)/dz^2 - d/dz[v_d c(z)] - [k_t n_t(z) + \lambda_b]c(z) + P(z,E) = 0 , \quad (1)$$

where $c(z)$ is the positron volume density at depth z, v_d is the field-dependent positron drift velocity, $n_t(z)$ is the atomic fraction of the defect density, k_t is the specific positron trapping rate, λ_b is the positron bulk annihilation rate, and D_+ is the positron diffusion coefficient related to the positron diffusion length by $L_+ = (D_+/\lambda_b)^{1/2}$. The most relevant parameter is the positron diffusion length which is sensitive to the presence of defects in the film. The positron implantation profile, used in the solution of this diffusion equation, is given by

$$P(z,E) = (m/z_0)(z/z_0)^{m-1}\exp[-(z/z_0)^m] , \quad (2)$$

where $z_0 = 1.13\bar{z}$, $\bar{z} = (\alpha_p/\rho)E^n$ is the mean implantation depth at energy E in keV, ρ is the density of the sample in g/cm^3,

$$\alpha_p = 3.32\ \mu\text{g/cm}^2\ \text{keV}^{1.6} ,$$

$m = 2$, and $n = 1.6$. In this analysis, the measured S parameters are represented by

$$S = \sum_l S_l f_l + S_{\text{surf}} f_{\text{surf}} , \quad (3)$$

where f_l is the fraction of the positrons in the lth layer, f_{surf} is the fraction of the positrons returning to the surface, S_l is the value of the S parameter characteristic of the lth layer, and S_{surf} is the S parameter for the surface.

Our results for the positron diffusion length range from 5 nm in the 1% CH_4 HFCVD film to 150 nm in the white diamond film (a range of 100 to 300 nm has been reported for natural diamond[16]). Using the measured positron diffusion lengths and a specific positron trapping rate of 10^{14} s^{-1}, we calculate the concentration of defects [number of defects (cm^{-3})/number of atomic sites (cm^{-3})] in each film; these range from about 0.13 in the 1% CH_4 HFCVD film to 6.8×10^{-5} in the white diamond film, respectively. The correlation between the FWHM of the Raman line of diamond and the positron diffusion length is clearly shown by the semilogarithmic plot in Fig. 5. Whereas the FWHM of the Raman line provides information about defect-free regions in the film via phonon scattering from defects such as twins, stacking faults, and dislocations, etc., the positron diffusion length is a direct measure of the atomic scale defects because of their deterministic effect on positron diffusion in the film. These data clearly show that the positron diffusion length is an order of magnitude more sensitive to defects than the FWHM of the diamond line in the Raman spectrum.

Nature of defects in the bulk

In order to understand better the nature of the defects, we have measured the positron lifetime spectra for regime-2 films that are relatively much thicker (8 to 25 μm) than regime-1 films. The regime-2 films, therefore, provide sufficient stopping power for the β-decay positrons from the ^{22}Na source. A typical positron lifetime spectrum is shown in Fig. 6. These spectra can be resolved into four exponentials and the results are plotted as functions of CH_4 concentration in Fig. 7. As stated above, the positron lifetime is a direct measure of the electron density at the site of the positron at the moment of annihilation. Knowledge about the nature of the defects is facilitated by the following identification: (1) the component of lifetime, $\tau_4 = 3.28 \pm 0.08$ ns represents pickoff annihilations of the triplet state of the positronium atom (o-Ps).[17] Since the positronium atom is not formed in the dense diamond lattice and/or even in monovacancies, this long-lived component reveals the existence of microvoids in the films. Although we cannot at present obtain the exact size of the microvoids, we can nonetheless estimate, by utilizing the known relationship between the o-Ps lifetime and the size of the voids in organic molecular solids,[18] a radius of about 4 Å for an assumed spherical shape of the microvoids. The constancy of τ_4 shows that the average size of the microvoids remains independent of CH_4 concentration, although its intensity (I_4) differs from film to film. The variations in I_4 reflect how the density of the microvoids changes in films that were deposited for different CH_4 concentrations in the HFCVD reactor. We argue in the following that this variation of the density of the microvoids is closely related to the competing growth rates for diamond and graphite in the films.

Another long-lived component of lifetime $0.82 < \tau_3 > 0.65$ ns represents o-Ps annihilations from different regions in the film. A shorter o-Ps lifetime in these regions means that either they are smaller in size than 4 Å, or the electron density in these regions is much higher than the electron density in the 4-Å-radius microvoids represented by τ_4. Additionally, whereas τ_4 remains constant for all regime-2 films, τ_3 changes as a function of CH_4 concentration. It is clear that these films contain two very different open-volume regions whose atomic scale dimen-

sions and electron densities can be probed by the positronium atom. In the following we argue that the size of the microvoid is not the only difference between these two microscopic regions. Otherwise, τ_3 and τ_4 should have behaved in a similar manner for all HFCVD films. We suggest that whereas τ_4 reveals microvoids of constant size and electron density, τ_3 represents graphite and/or amorphous regions in the films. Since the electron density in these latter regions is expected to be much higher than that in the open-volume microvoids, τ_3 should be, in agreement with our observation, smaller than τ_4. Thus, as the CH_4 concentration is increased from 0.25% to 2%, the relative abundance of the graphitic and/or amorphous regions increases (as confirmed by

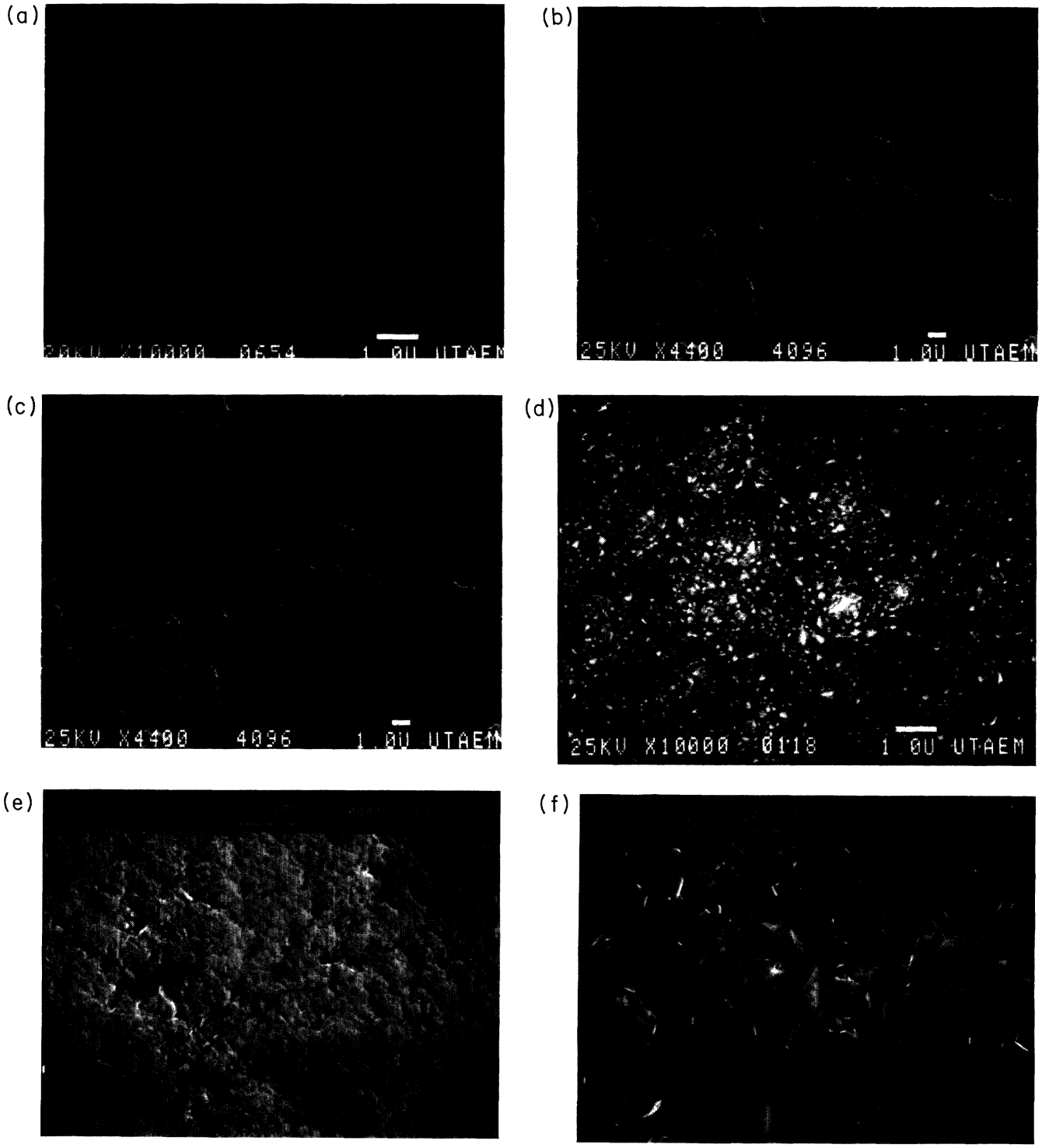

FIG. 3. Typical SEM micrographs for different diamond films: (a) 0.25% CH_4 of regime 1, (b) 2% CH_4 of regime 1, (c) 1% CH_4 of regime 2, (d) 2.5% CH_4 of regime 2, (e) white diamond of plasma arc jet, and (f) black diamond of plasma arc jet.

the Raman data, for example) and, consequently, τ_3 decreases. Under these conditions, the relative intensity I_3 should be a direct measure of the density of the graphitic and/or amorphous regions in the films. This is confirmed by a linear relationship (Fig. 8) between I_3 and the sum of the intensities of the 1350 and 1580-cm^{-1} Raman lines that are characteristic of the sp^2-bonded graphitic regions.

The component of lifetime $\tau_2=(0.243\pm0.002)$ ns and $I_2=(75.8\pm1.0)\%$ that remains independent of CH_4 concentration originates primarily from positrons trapped in monovacancies in the film. That τ_2 represents vacancies in the film can be established only after resolving the following issue: Could this component be due to the annihilations of positrons in the silicon substrate on which the HFCVD films were deposited? This possibility will yield a component with a mean lifetime between 0.22 ns and 0.27 ns that are known to be the lifetimes of positrons annihilating in crystalline silicon and vacancy in silicon, respectively.[19] We have measured vacancy concentrations on the order of 10^{-6} in similar Czochralski-grown silicon wafers.[19] It is conceivable that such low levels of defects could have been produced in the substrate during the early stages of the growth of the film while the silicon substrate was continuously bombarded with the hydrocarbon radicals and hydrogen. What makes matters even more complex is the fact that the substrates used in the HFCVD growth were usually boron-doped p-typed silicon in which the positron lifetime is 0.245 ns.[20] It is therefore possible that τ_2 represents contributions from the annihilations of the positrons in the p-type silicon substrate, vacancies in the silicon substrate, and diamond. That the component of lifetime τ_2 originates primarily from annihilations in the diamond film, as opposed to annihilations in the silicon substrate, is supported by our observation that the intensity of this lifetime component (I_2), measured for a number of films, does not change significantly even though the film thickness is in-

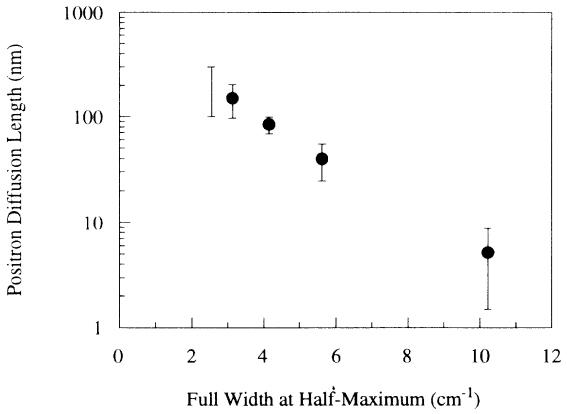

FIG. 5. The positron diffusion length vs FWHM of the 1332-cm^{-1} Raman peak for HFCVD and plasma arc jet films. The positron diffusion length for natural diamond is taken from Ref. 16.

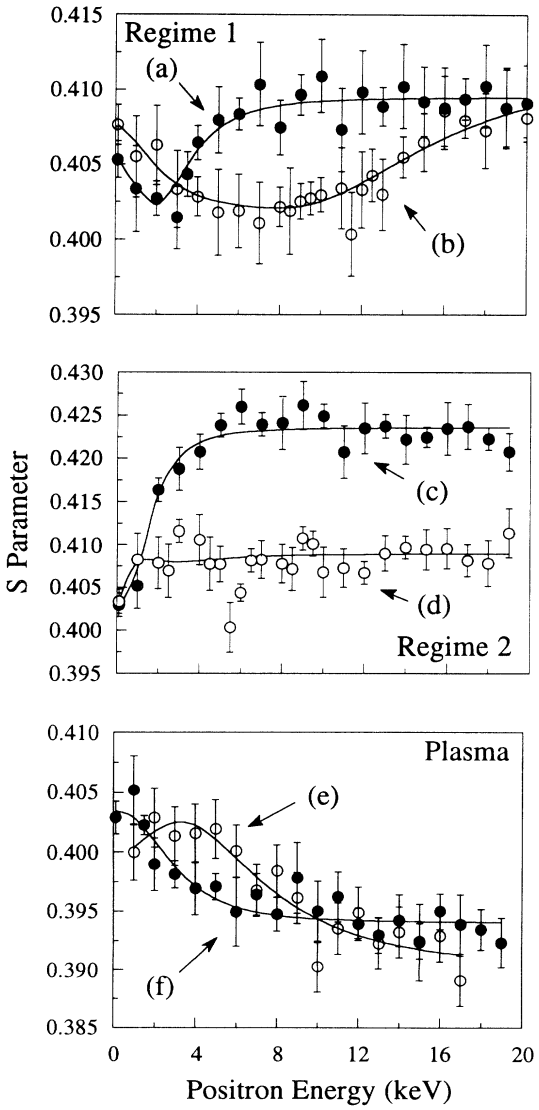

FIG. 4. The S parameter vs positron implantation energy for HFCVD and plasma arc jet films: (a) 2% CH_4, regime 1; (b) 0.25% CH_4, regime 1; (c) 4% CH_4, regime 2; (d) 1% CH_4, regime 2; (e) white diamond; and (f) black diamond. The solid curves represent weighted least-squares fits of the positron diffusion equation (1).

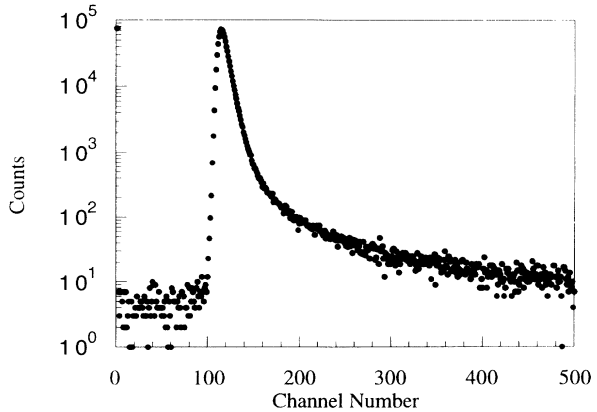

FIG. 6. Typical positron lifetime spectrum measured for diamond film grown for 1% CH_4 of regime 2.

creased from 8 to 25 μm. If this lifetime component had any significant contribution from the substrate, then its lifetime τ_2 and/or intensity I_2 would exhibit a change as the number of the positrons reaching the substrate diminishes with increasing thickness of the diamond film. In order to resolve this issue, clearly, we have measured the positron lifetime spectrum for a self-standing and thick arc jet produced diamond film whose thickness ($\sim$500

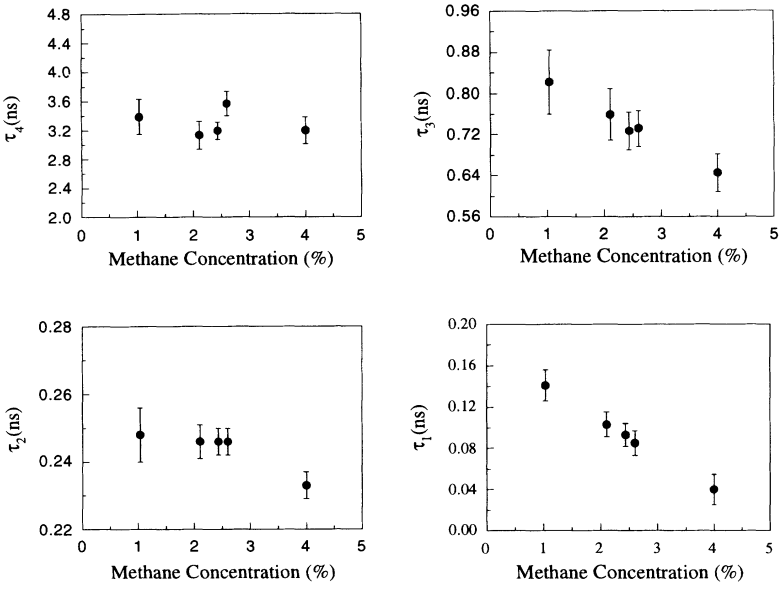

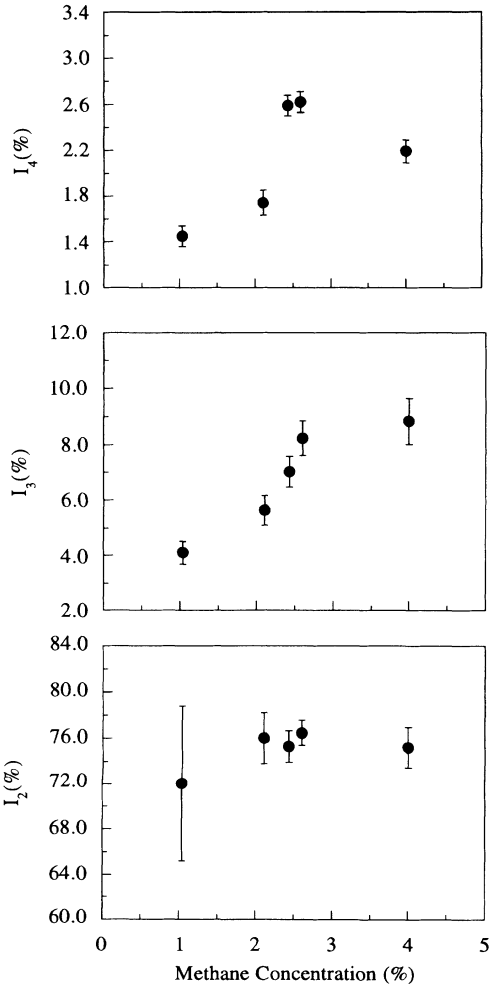

FIG. 7 . Positron lifetimes and relative intensities vs CH_4 concentration for the HFCVD films.

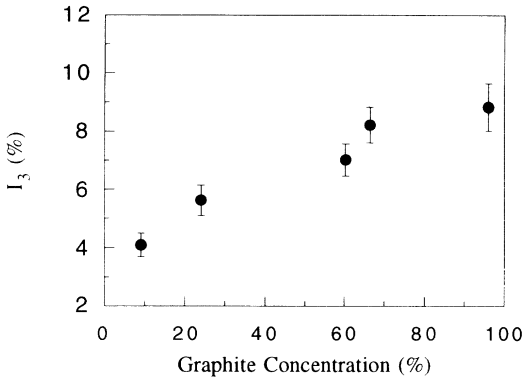

FIG. 8. Relative intensity I_3 vs sum of the intensities of the 1350 and 1580 cm^{-1} Raman peaks.

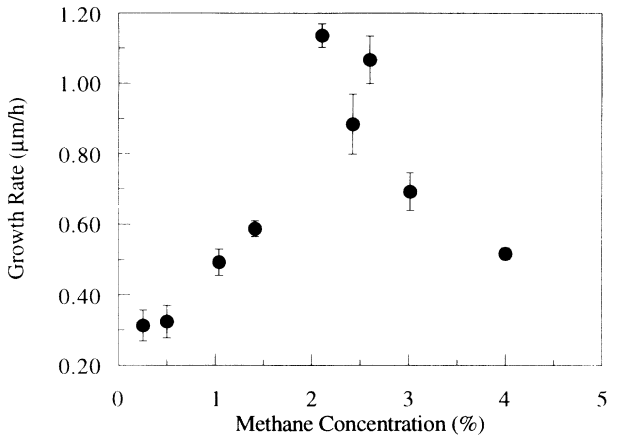

FIG. 9. Average growth rate vs CH_4 concentration for regime-2 films.

μm) is several times the maximum penetration depth of the ^{22}Na positrons. Again, in the lifetime spectrum of this self-standing and sufficiently thick diamond sample, we have resolved four lifetime components with $\tau_1=(0.08\pm0.003)$ ns; $\tau_2=(0.23\pm0.02)$ ns, $I_2=(24.7\pm1.1)\%$; $\tau_3=(0.53\pm0.09)$ ns, $I_3=(4.3\pm1.5)\%$; and $\tau_4=(2.10\pm0.20$ ns, $I_4=(1.8\pm0.2)\%$. These results are in good agreement with those obtained for the regime-2 diamond films. They strongly support the validity of the four lifetime components resolved in the HFCVD films and further show that the lifetime component τ_2 for the regime-2 films arises from annihilations in the diamond film. In spite of markedly different growth parameters, the HFCVD and plasma arc jet grown films contain microvoids (represented by τ_4), amorphous regions (represented by τ_3), and vacancies (represented by τ_2). Apparent differences in the sizes of the microvoids and defect densities between the diamond films grown by these two techniques are not surprising. The lifetime of the shortest-lived component τ_1 in the 1% CH_4 HFCVD film is (0.140 ± 0.015) ns. This agrees reasonably well with (0.131 ± 0.004) ns, measured previously for a different CVD film[9] and is to be compared with the positron lifetime of 0.116 ns in crystalline diamond. The decrease in τ_1 with increasing CH_4 concentration reflects, in accordance with the two-state trapping model,[21] positron trapping by an increasing concentration of defects in the films. The behavior of τ_1, therefore, reflects changes in the defect density for the regime-2 diamond films.

Film growth versus defects

In order to gain an insight into the growth process, we plot in Fig. 9 the average growth rate, obtained from profilometer measurements, vs CH_4 concentration for regime-2 films. These data are consistent with a competition between the relative growths of the sp^3-bonded diamond and sp^2-bonded graphitic structures in the films. As shown clearly by the Raman and SEM measurements, the films deposited for low CH_4 concentrations are rich in the sp^3-bonded diamond structure and they are characterized by a relatively low growth rate. With increasing methane concentration up to about 2.5%, the sp^2-bonded graphitic structure is favored and it develops with an increasing growth rate. For CH_4 concentrations $>2.5\%$, the competing processes must balance so as to produce a predominantly sp^2-bonded structure at slower growth rates. The average growth rate of the HFCVD films and the density of the microvoids (reflected by I_4) exhibit a strikingly similar behavior with CH_4 concentration. Both increase with increasing CH_4 concentration, reach their respective maximum $\sim2.5\%$ CH_4, and decline for higher CH_4 concentrations. Clearly, the average growth rate and the density of the microvoids are closely related. This correlation is further supported by the S parameter measured for the HFCVD films by using the beta-decay positrons from a ^{22}Na source. These data are shown in Fig. 10 and they are consistent with a change in the quality (high vs low crystalline order) of the film as CH_4 concentration is varied. It is seen that the S parameter increases from (0.425 ± 0.001) to (0.442 ± 0.001) as CH_4 concentration is increased from 1% to 2.5%. Beyond this concentration, the S parameter turns over and de-

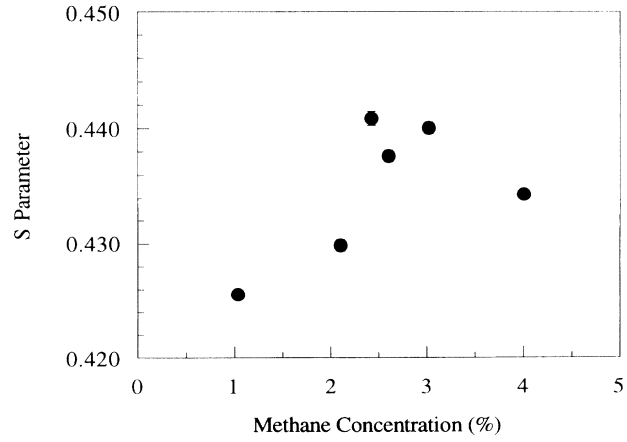

FIG. 10. The S parameter vs CH_4 concentration for the HFCVD films.

creases to about 0.435 at 4% CH_4 concentration. It is well established that the S parameter increases upon positron trapping in defects. The initial increase in the S parameter is thus a reflection of an increasing concentration of defects as the films evolve from a purely diamond material to another containing both diamond and graphite. The following decrease in the S parameter indicates a decreasing defect density as the films change from a mixed phase of diamond and graphite to a purer graphitic sample. The fact that the S parameter for the 1% CH_4 film is lower than the S parameter for the 4% CH_4 film shows that the almost purely diamond film is of higher crystalline quality than the mainly graphitic material. Similar correlations between the growth rate and defect density have been seen previously with use of totally different techniques.[22]

IV. CONCLUSIONS

In conclusion, we have presented results on microstructural defects in HFCVD and plasma arc jet diamond films; these films contain vacancies, microvoids, and graphitic and/or amorphous regions with concentrations ranging from 0.13 to 6.8×10^{-5}. We have presented evidence for important correlations between defects and growth rate and properties of the films. The best quality diamond film has the lowest growth rate and also the lowest density of the microvoids. The film grown at the highest rate also develops a much higher density of the microvoids. The FWHM of the 1332-cm^{-1} Raman peak has been correlated, for the first time, with the positron diffusion length in diamond films. The positron diffusion length is much more sensitive to the presence of defects than the FWHM of the 1332-cm^{-1} Raman line.

*Present address: Loral Vought, Dallas, Texas 75265.
†To whom all correspondence should be addressed.

[1]See excellent papers in, *Thin Film Diamond,* edited by A. H. Lettington and J. W. Seeds [Philos. Trans. Phys. Sci. Eng. **342**, 193 (1993)]; in *New Diamond Sciences and Technology,* edited by R. Messier, J. T. Glass, J. Butler, and R. Roy, MRS Symposia Proceedings (Materials Research Society, Pittsburgh, 1990).

[2]J. M. Perez, C. Lin, W. Rivera, R. C. Hyer, M. Green, S. C. Sharma, D. R. Chopra, and A. R. Chourasia, Appl. Phys. Lett. **62**, 1889 (1993).

[3]R. C. Hyer, M. Green, K. K. Mishra, and S. C. Sharma, J. Mater. Sci. Lett. **10**, 515 (1991).

[4]S. C. Sharma, M. Green, R. C. Hyer, C. A. Dark, T. D. Black, A. R. Chourasia, D. R. Chopra, and K. K. Mishra, J. Mater. Res. **5**, 2424 (1990).

[5]A. R. Chourasia, D. R. Chopra, S. C. Sharma, M. Green, C. A. Dark, and R. C. Hyer, Thin Solid Films **193/194**, 1079 (1990).

[6]S. C. Sharma, C. A. Dark, R. C. Hyer, M. Green, T. D. Black, A. R. Chourasia, D. R. Chopra, and K. K. Mishra, Appl. Phys. Lett. **56**, 1781 (1990).

[7]G. Kogel, D. Schodlbauer, W. Triftshauser, and J. Winter, Phys. Rev. Lett. **60**, 1550 (1988).

[8]A. Uedono, S. Tanigawa, H. Funamoto, A. Nishikawa, and K. Takohashi, Jpn. J. Appl. Phys. **29**, 555 (1990).

[9]S. Dannefaer, T. Bretagnon, and D. Kerr (unpublished).

[10]P. Kirkegaard and M. Eldrup, Comput. Phys. Commun. **1**, 401 (1974).

[11]*Positron Solid State Physics,* edited by W. Brandt and A. Dupasquier (North-Holland, Amsterdam, 1983).

[12]R. E. Shroder, R. J. Nemanich, and J. T. Glass, Phys. Rev. B **41**, 3738 (1990).

[13]L. H. Robins, E. N. Farabaugh, and A. Feldman, J. Mater. Res. **5**, 2456 (1990).

[14]S. C. Sharma, N. Hozhabri, R. C. Hyer, T. Hossain, S. Kim, F. O. Meyer III, M. F. Pas, and A. E. Stephens, in *Defect Engineering in Semiconductor Growth, Processing and Device Technology,* edited by S. Ashok, J. Chevallier, K. Sumino, and E. Weber, MRS Symposia Proceedings No. 262 (Materials Research Society, Pittsburgh, 1992), p. 45.

[15]A. van Veen, H. Schut, J. de Vries, R. A. Hakvoort, and M. R. Ijpma, in *Positron Beams for Solid Surfaces,* edited by P. J Schultz, G. R. Massoumi, and P. J. Simpson, AIP Conf. Proc. No. 218 (AIP, New York, 1990).

[16]R. M. Nieminen and M. J. Maninen, in *Positrons in Solids,* edited by P. Hautojarvi, Springer Topics in Current Physics Vol. 12 (Springer Verlag, Berlin, 1979).

[17]S. C. Sharma, in *Positron and Positronium Chemistry,* edited by D. M. Schrader and Y. C. Jean (Elsevier, New York, 1988), pp. 193–239.

[18]M. Eldrup, in *Positron Annihilation,* edited by P. G. Coleman, S. C. Sharma, and L. M. Diana (North-Holland, Amsterdam, 1982).

[19]S. C. Sharma, R. C. Hyer, N. Hozhabri, M. F. Pas, and S. Kim, Appl. Phys. Lett. **61**, 1939 (1992).

[20]P. Sen and C. Sen, J. Phys. C **7**, 2776 (1974).

[21]W. Brandt, in *Positron Annihilation,* edited by A. T. Stewart and L. O. Roellig (Academic, New York, 1967).

[22]B. E. Williams and J. T. Glass, J. Mater. Res. **4**, 373 (1989).

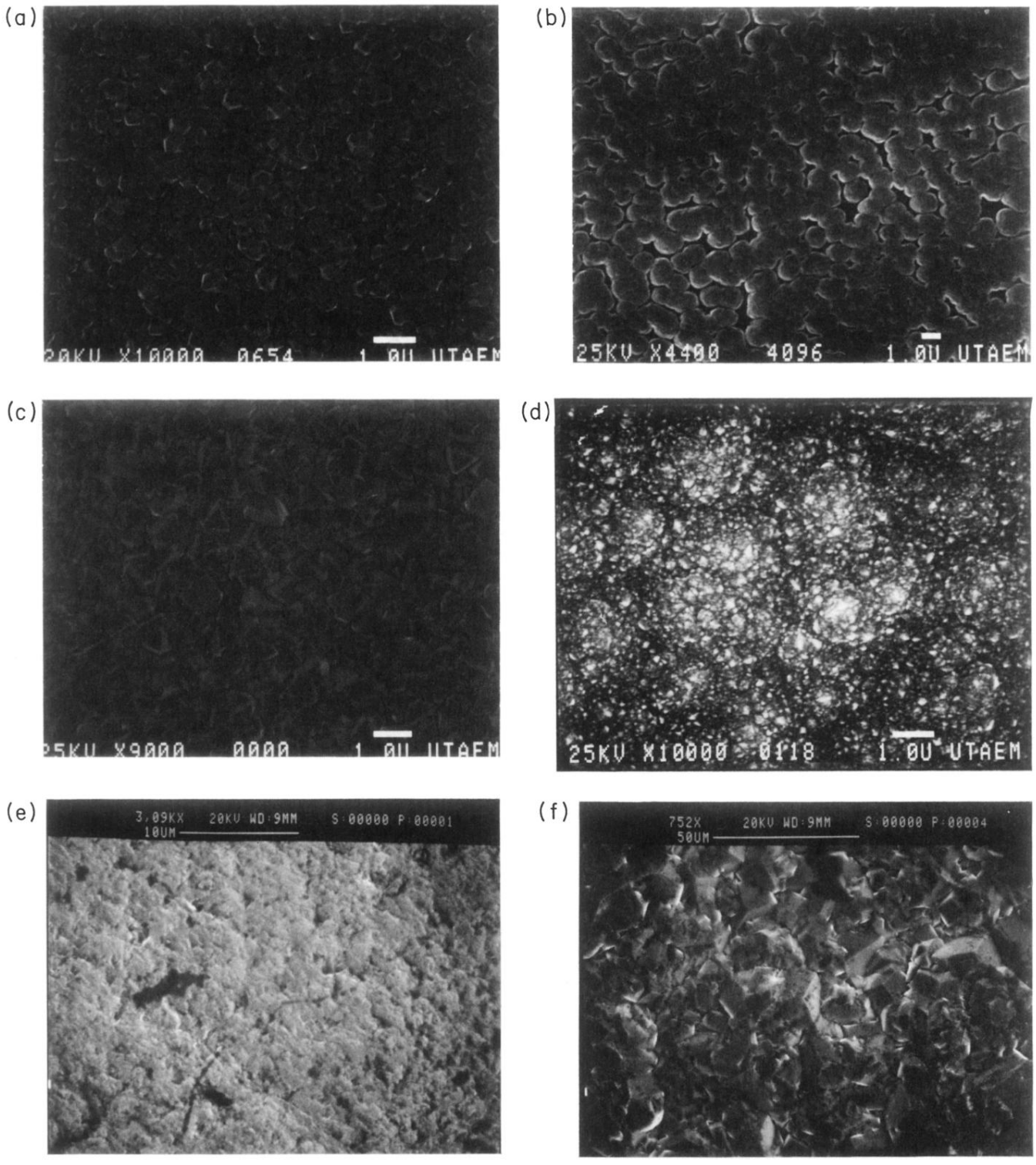

FIG. 3. Typical SEM micrographs for different diamond films: (a) 0.25% CH_4 of regime 1, (b) 2% CH_4 of regime 1, (c) 1% CH_4 of regime 2, (d) 2.5% CH_4 of regime 2, (e) white diamond of plasma arc jet, and (f) black diamond of plasma arc jet.